BAD and glucokinase reside in a mitochondrial complex that integrates glycolysis and apoptosis

Nika N. Danial[1], Colette F. Gramm[1], Luca Scorrano[1]*, Chen-Yu Zhang[2], Stefan Krauss[2], Ann M. Ranger[1], Sandeep Robert Datta[3], Michael E. Greenberg[3], Lawrence J. Licklider[4], Bradford B. Lowell[2], Steven P. Gygi[4] & Stanley J. Korsmeyer[1]

[1]*Howard Hughes Medical Institute, Dana-Faber Cancer Institute, Harvard Medical School, Boston, Massachusetts 02115, USA*
[2]*Division of Endocrinology, Beth Israel Deaconess Medical Center, Harvard Medical School, Boston, Massachusetts 02215, USA*
[3]*Division of Neuroscience, Children's Hospital, Department of Neurobiology, Harvard Medical School, Boston, Massachusetts 02115, USA*
[4]*Department of Cell Biology, Taplin Biological Mass Spectrometry Facility, Harvard Medical School, Boston, Massachusetts 02115, USA*

* Present address: Venetian Institute of Molecular Medicine, Padova 35129, Italy

Glycolysis and apoptosis are considered major but independent pathways that are critical for cell survival[1–4]. The activity of BAD, a pro-apoptotic BCL-2 family member, is regulated by phosphorylation in response to growth/survival factors[5–8]. Here we undertook a proteomic analysis to assess whether BAD might also participate in mitochondrial physiology. In liver mitochondria, BAD resides in a functional holoenzyme complex together with protein kinase A[7] and protein phosphatase 1 (PP1) catalytic units[9], Wiskott–Aldrich family member WAVE-1 as an A kinase anchoring protein[10], and glucokinase (hexokinase IV)[11]. BAD is required to assemble the complex in that *Bad*-deficient hepatocytes lack this complex, resulting in diminished mitochondria-based glucokinase activity and blunted mitochondrial respiration in response to glucose. Glucose deprivation results in dephosphorylation of BAD, and BAD-dependent cell death. Moreover, the phosphorylation status of BAD helps regulate glucokinase activity. Mice deficient for BAD or bearing a non-phosphorylatable BAD(3SA) mutant[12] display abnormal glucose homeostasis including profound defects in glucose tolerance. This combination of proteomics, genetics and physiology indicates an unanticipated role for BAD in integrating pathways of glucose metabolism and apoptosis.

Multidomain pro-apoptotic BCL-2 members BAX and BAK constitute a requisite gateway to the mitochondrial pathway of apoptosis, and their allosteric activation results in permeabilization of the outer mitochondrial membrane[4,13]. BH3-only molecules including BAD, BID, NOXA and BIM are connected to proximal death and survival signals, and can result in the activation of BAX and BAK or can be sequestered by anti-apoptotic BCL-2 and BCL-X_L[14]. Kinases that phosphorylate and inactivate BAD have been shown to localize to mitochondrial membranes, and depending on cellular context include mitochondria-tethered protein kinase A (PKA) for S112 and S155 sites in response to interleukin-3 (IL-3), and a mitochondria-based component of p70S6 kinase for S136 after insulin-like growth factor (IGF)-I signalling (refs 6–8).

To assess whether BAD and perhaps enzymes responsible for its modification reside in higher-order protein complexes at the mitochondria, we performed gel filtration chromatography. Conditions for fractionation were established using mitochondria purified from the haematopoietic cell line FL5.12 expressing BAD and BCL-X_L (Supplementary Fig. 1). To examine the fractionation profile of endogenous BAD within normal tissue, Percoll centrifugation was used to separate mouse liver mitochondria from other cellular membranes. Purified mitochondria were solubilized in CHAPS, a zwitterionic detergent that does not alter the conformation of BCL-2 family proteins[15]. We initially used mild conditions (1 mM CHAPS) to keep peripheral protein complexes intact, followed by Superose 6 gel filtration (Fig. 1a). Immunoblots of gel-excluded fractions revealed that BAD_L (28 kDa) and BAD_S (23 kDa) isoforms were present within complexes of 25–669 kDa in mouse liver mitochondria and that the BAD_S species predominated (Fig. 1b). The fractionation properties of BAD remained the same when mitochondria were solubilized in 1, 6 or 15 mM (1%) CHAPS (critical micelle concentration about 6–10 mM) (Supplementary Fig. 2). In 1–15 mM CHAPS the fractionation properties of VDAC, the outer mitochondrial membrane import receptor Tom20, the import channel Tom40 and the mitochondrial chaperone Hsp60 are distinct and consistent with published observations[16,17].

BAD-containing fractions from gel filtration were separated under non-denaturing conditions, revealing multiple silver-stained protein complexes (Fig. 1c). Immunoblots of these second dimension native gels revealed BAD immunoreactivity within distinct complexes in fractions C to E2 from liver mitochondria (Fig. 1d). Gel-excluded proteins (first dimension), which were fractionated into native complexes under non-denaturing conditions (second dimension), were subsequently separated into their individual components (third dimension) by placing a native gel slice horizontal as a stack above an SDS–polyacrylamide gel electrophoresis (PAGE) denaturing gel (Fig. 1a). Silver stains of third dimension gels (Fig. 1e) revealed the individual protein constituents of each native complex (Fig. 1c). Third dimension gels were also transferred and immunoblotted, confirming the presence of 23-kDa BAD_S, but not BAD_L, in an approximately 232-kDa complex (Fig. 2a). Five potential component proteins of a roughly 232-kDa BAD-containing complex were consistently present in silver-stained third dimension gels of fractions D to E2 (Fig. 1e, red arrows). Moreover, immunoblots using an antibody specific for the phosphorylated S112 site of BAD indicate that at least a portion of BAD_S present within this complex is phosphorylated (data not shown). The absence of an immunoreactive complex in *Bad*-deficient liver mitochondria (Fig. 2a) confirmed the specificity of the BAD-containing complex. In contrast, manganese SOD localized in complex(es) ranging from about 158 to 232 kDa in $Bad^{-/-}$ as well as $Bad^{+/+}$ mitochondria, indicating that only BAD-specific complexes were disrupted in the *Bad* knockout liver (Fig. 2a).

The approximately 232-kDa native protein complexes isolated from second dimension gels (Fig. 1c) and individual protein species excised from third dimension gels (Fig. 1e) were sequenced by liquid chromatography tandem mass spectrometry (LC-MS/MS), which identified a peptide that is 94% identical to the catalytic subunit of human PP1α and rat PP1α serine/threonine phosphatase. Its precise identity as the 36-kDa catalytic subunit (PP1c) was confirmed by immunoblot of a third dimension gel (Fig. 2a). The correctly sized BAD_S, $PP1_C$ and PKAc vertically align on third dimension gels, supporting their presence together within a complex of roughly 232 kDa (Fig. 2a).

A second approach to assess whether candidate proteins resided together in a complex used immunoprecipitation of fractions from FL5.12 mitochondria, revealing that BAD_S and PKA_C precipitated together with $PP1_C$ (Supplementary Fig. 1c). As a third assessment of whether candidate proteins associate, we isolated $PP1_C$-interacting proteins by microcystin affinity chromatography, which efficiently purifies $PP1_C$ owing to its high-capacity binding to this phosphatase[9]. Microcystin-Sepharose affinity pull-downs revealed multiple proteins, and immunoblots confirmed the purification of $PP1_C$ (Fig. 2b). Another closely related phosphatase with microcystin-binding capacity, namely PP2A, was not present (Supplementary Fig. 3). PKA_C and BAD_S also co-purified with the captured PP1 from wild-type mitochondria (Fig. 2b), supporting all other evidence showing their presence together in a mitochondrial complex.

Confocal microscopy of mouse embryonic fibroblasts (MEFs) demonstrated that $PP1_C$ localizes together with Tom20 (Fig. 2d). Submitochondrial fractionation of mouse liver mitochondria confirmed that PP1 is detected in the mitochondrial outer membrane fraction (data not shown). The presence of PP1 at mitochondria was not expected[18]. Our data indicate that a portion of phosphorylated BAD is present at mitochondria, supporting opposing kinase and phosphatase activities as part of the same BAD-containing multienzyme complex.

To test the role of PP1 in BAD dephosphorylation we used a PP1-blocking peptide known to inhibit subcellular targeting of PP1 and its dephosphorylation activity on substrates[19]. Addition of the R/K-X-V/I-X-F motif containing blocking peptide to mitochondria of FL5.12 cells, prepared immediately after their withdrawal from IL-3, prevented the dephosphorylation of BAD, but the mutant F68A peptide did not (Fig. 2e; see also Supplementary Fig. 4). Of note, the requirement for $>10^{-6}$ M okadaic acid to inhibit the phosphatase activity for mitochondrial BAD indicates the participation of PP1, not PP2A (Supplementary Fig. 4). These approaches support a model in which PP1 is specifically targeted to mitochondria where it resides in an enzyme complex responsible for the dynamic dephosphorylation of BAD.

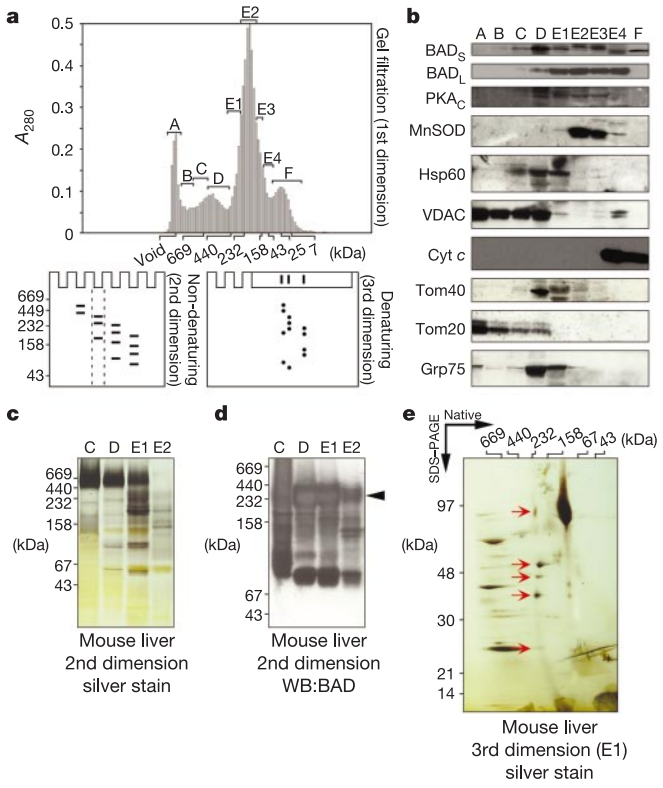

Figure 1 Characterization of mitochondrial complexes containing BAD. **a**, Schematics depicting the first, second and third dimension separation of mitochondrial protein complexes. Top panel, elution profile of mitochondrial proteins. Mitochondria isolated from mouse liver were solubilized in 1 mM CHAPS, subjected to gel filtration on Superose 6, and 200-μl fractions were collected. Protein concentration is plotted to identify elution peaks. A_{280}, absorbance at 280 nm. **b**, Fifty micrograms of pooled fractions were loaded onto an 8–16% gradient SDS–PAGE and immunoblotted with the indicated antibodies. MnSOD, manganese SOD. **c**, **e**, Representative silver stain of second (**c**) and third (**e**) dimension gel fractionation of mitochondrial complexes, that were subsequently subjected to LC-MS/MS. Arrows in **e** indicate five components of an approximately 232-kDa complex consistently noted on third dimension analysis. **d**, Native BAD-containing complexes of mouse liver mitochondria. One hundred and fifty micrograms of gel-filtrated liver mitochondrial fractions were subjected to non-denaturing electrophoresis (second dimension). Proteins were transferred and immunoblotted (WB) with an anti-BAD antibody. Arrow indicates the most prominent BAD complex.

The presence of PKA and PP1 suggested that the complex might possess an A kinase anchoring protein (AKAP). Whereas D-AKAP1 had been noted at the mitochondria of FL5.12 cells[7], LC-MS/MS of the approximately 232-kDa native complexes from liver identified WAVE-1, a member of Wiskott–Aldrich family proteins[20]. In addition to regulating actin polymerization, WAVE-1 functions as an AKAP, binding the PKA regulatory subunit (RII)[10]. An RII overlay as well as immunoblots performed on a third dimension gel recognized approximately 232, 134 and 67-kDa species, implicating WAVE-1 as the AKAP within these mitochondrial complexes (Fig. 2f). Moreover, WAVE-1 aligned vertically with BAD_S and $PP1_C$ on a third dimension gel, evidence indicating that they resided in a BAD-containing complex (Fig. 2f). Further evidence that WAVE-1 resided within this holoenzyme complex was provided by its presence in microcystin pull-downs of $PP1_C$ (Fig. 2b; see also Supplementary Fig. 3). Immunoprecipitation of mitochondrial proteins solubilized in 15 mM CHAPS revealed that WAVE-1 precipitated together with BAD, providing a third approach to confirm their association (Fig. 2c). Immunoelectron microscopy using an antibody to WAVE-1 revealed prominent decoration of the outer mitochondrial membrane (Fig. 2g). Immunolocalization studies using confocal microscopy indicated a portion of WAVE-1 localized with Tom20 at the mitochondria (Supplementary Fig. 5).

To assess whether the BAD-containing complex at mitochondria actually required BAD for its assemblage, we performed a similar first, second and third dimension analysis on the mitochondria from livers of *Bad*-deficient mice. Immunoblots of third dimension gels from fractions D through to E2 failed to detect any $PP1_C$, PKA_C, WAVE-1 or BAD (Fig. 2a, f). An examination of multiple fractions indicates that deletion of BAD results in disassembly of the entire protein complex rather than a shift to a slightly smaller-sized complex. This suggests that BAD also functions as a scaffold to nucleate the proper architecture of this complex, as well as being a substrate for the kinase–phosphatase pair localized to this microenvironment.

The components BAD_S (23 kDa), PKA_C (41 kDa), $PP1_C$ (36 kDa) and WAVE-1 (85-kDa isoform) do not account for the approximately 50-kDa protein noted by silver stain on the third dimension gel of the approximately 232-kDa core complex (Fig. 1e). LC-MS/MS analysis of the PP1-associated proteins captured from liver mitochondrial lysates identified glucokinase (Fig. 2b; see also Supplementary Fig. 3), a 52-kDa protein whose expression pattern is mainly restricted to liver and β-islet cells[11,21]. An immunoblot of the microcystin pull-down confirmed that glucokinase precipitated together with $PP1_C$, BAD_S, PKA_C and WAVE-1 (Fig. 2b, see also Supplementary Fig. 3). Moreover, an immunoprecipitation of glucokinase from 15 mM CHAPS-solubilized mitochondria also precipitated together with WAVE-1, BAD_S and PKA_C (Fig. 2c). Further evidence that glucokinase was a component of the approximately 232-kDa complex was provided by immunoblots of third dimension gels where glucokinase aligned vertically with BAD_S, PKA_C and $PP1_C$ (Fig. 2a).

Absence of the approximately 232-kDa complex containing glucokinase in $Bad^{-/-}$ cells prompted an assessment of the physiological consequence of losing the mitochondria-tethered component of this enzyme. The rate of organelle-based glucokinase activity was severely blunted in $Bad^{-/-}$ compared with wild-type liver mitochondria (Fig. 3a, $P < 0.01$), indicating that a localized enzymatic defect resulted from the loss of a focused glucokinase complex. An immunoblot comparing purified mitochondria and cytosol from hepatocytes confirmed a decrease in glucokinase protein in $Bad^{-/-}$ mitochondria (Fig. 3b).

Although glucokinase activity at the surface of *Bad*$^{-/-}$ mitochondria was markedly diminished (Fig. 3a), most of the glucokinase resides in the cytosol (Fig. 3b). This prompted us to ask whether intact cells from these mice would exhibit a specific defect in the use of glucose as a respiratory substrate. Addition of glucose to wild-type hepatocytes increased the rate of oxygen consumption, whereas respiration driven by glucose in *Bad*$^{-/-}$ hepatocytes was significantly compromised, as depicted by the slope of the oxygen consumption curve (Fig. 3c). Consistent with this, the percentage increase in ATP after treatment with glucose was also decreased in *Bad*$^{-/-}$ hepatocytes (data not shown). If the purpose of BAD-dependent, mitochondrial-tethered glucokinase is to provide this organelle directly with metabolic intermediates to drive mitochondrial processes including respiration, then the respiration of *Bad*$^{-/-}$ hepatocytes might be corrected by substituting pyruvate, a downstream product of glycolysis. Addition of exogenous pyruvate to digitonin-permeabilized *Bad*$^{-/-}$ hepatocytes restored the oxygen consumption rate to that of wild-type cells (Fig. 3c, d). Moreover, respiration in response to an alternative carbon source, fructose, was also equivalent in *Bad*$^{-/-}$ cells (Fig. 3d). Thus, the respiratory complexes in *Bad*$^{-/-}$ liver seem intact, strongly supporting the role of a BAD-dependent multiprotein complex in the usage of glucose at mitochondria.

As glucose metabolism is linked to cell survival[2,3], we assessed BAD phosphorylation in the presence or absence of glucose. BAD S112 was phosphorylated when glucose was present but not when it was absent from the medium of a hepatocyte cell line (Fig. 3e). Addition of glucose to purified liver mitochondria induced the phosphorylation of BAD (Fig. 3e). Moreover, the absence of BAD markedly protected liver cells from apoptosis when deprived of glucose (Fig. 3f).

Mutations in glucokinase have been associated with maturity-onset type 2 diabetes of the young[11]. Similar defects in glucose regulation have been recapitulated in mice with genetic alterations in the glucokinase gene[21,22], prompting us to examine whether BAD has an effect on glucose homeostasis. Blood glucose measurements in fed and fasted mice revealed a substantial fasting hyperglycaemia (28% increase, $P < 0.05$, Fig. 3g) as well as a fed hyperinsulinaemia (not shown) in *Bad*$^{-/-}$ mice. After intraperitoneal injection of glucose (1 g glucose per kg mouse), *Bad*$^{-/-}$ mice showed a significant defect in the rate of blood glucose clearance (Fig. 3h).

As glucose could regulate the phosphorylation of BAD in hepatocytes (Fig. 3e), we tested whether the phosphorylation status of BAD affected the mitochondrial complex. We examined hepatocytes from a 'knockin' mouse bearing a non-phosphorylatable BAD(3SA) molecule in which the three regulatory serines (S112, S136 and S155) were converted to alanine[12]. Although BAD protein is required to nucleate this mitochondrial complex (Fig. 2a), the phosphorylation of BAD is not required as BAD(3SA) liver contained the multiprotein complex, as demonstrated by third dimension analysis (Fig. 4a) and microcystin pull-down (Fig. 2b). However, despite normal amounts of mitochondrial glucokinase protein, the glucokinase activity was markedly blunted in

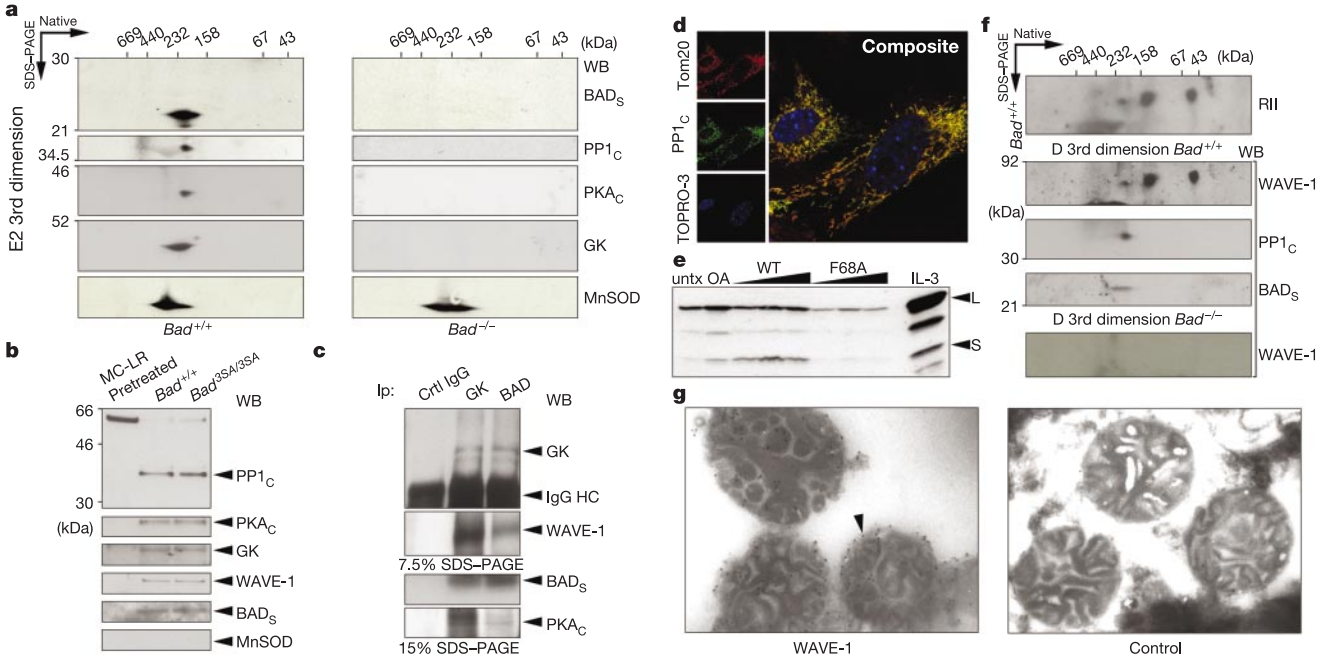

Figure 2 Components of a mitochondrial BAD complex. **a**, Immunoblot of third dimension gel of a mitochondrial protein complex from the liver of *Bad*$^{+/+}$ and *Bad*$^{-/-}$ mice. GK, glucokinase. **b**, Microcystin affinity purification of PP1-interacting proteins in mouse liver mitochondria. Mitochondria solubilized in 15 mM CHAPS were incubated with microcystin-coupled Sepharose (MC-Sepharose) beads and bound proteins were resolved by SDS–PAGE and immunoblotted (WB) with the indicated antibodies. Pretreatment of mitochondrial lysates with microcystin serves as a control. **c**, Co-immunoprecipitation of BAD_S, glucokinase, WAVE-1 and PKA_C. Mouse liver mitochondrial proteins solubilized in 15 mM CHAPS were immunoprecipitated (IP) with an antibody to BAD or glucokinase, immunoprecipitates were resolved on 7.5% or 15% SDS–PAGE gels and immunoblots were developed with the indicated antibodies. IgG HC, immunoglobulin-γ heavy chain. **d**, Immunolocalization of PP1 to mitochondria by confocal microscopy of MEFs revealing co-localization with Tom20. **e**, PP1 targeting inhibitor prevents BAD dephosphorylation. Purified mitochondria from FL5.12 cells deprived of IL-3 were incubated with 10–1,000 nM wild-type (WT) or mutant (F68A) peptide[19], and BAD phosphorylation on S112 was examined. OA, okadaic acid. **f**, RII-binding activity within the BAD complex. A third dimension gel of filtrated fraction D from wild-type liver mitochondria was analysed by an RII overlay assay[19] or immunoblot. An immunoblot of the third dimension gel of fraction D from *Bad*$^{-/-}$ liver mitochondria was also developed for WAVE-1. **g**, Immunogold decoration of mitochondria by a WAVE-1 antibody (arrowhead) as detected by immunoelectron microscopy of thin sections from purified liver mitochondria.

BAD(3SA) mitochondria (Fig. 4b, $P < 0.001$). Moreover, mitochondrial glucokinase activity was substantially inhibited by a PKA inhibitor (H-89) (Fig. 4c) or a PKA-specific inhibitory peptide (PKI) (not shown), both of which blocked S112 phosphorylation[7]. Finally, we examined *Bad*$^{3SA/3SA}$ mice *in vivo*, revealing a comparable defect in glucose homeostasis to that in *Bad*$^{-/-}$ mice. This includes significant fasting hyperglycaemia (Fig. 4d) as well as a marked defect in blood glucose clearance (Fig. 4e). These findings provide genetic evidence that BAD phosphorylation helps to regulate glucose homeostasis.

Cells depend on the availability of growth/survival factors that characteristically regulate both cellular metabolism and cell survival. Insulin, IGF-I and multiple cytokines transduce signals via phosphatidylinositol-3-OH kinase through AKT and related kinases, which maintain glucose transport (Glut) and recruit hexokinase to mitochondria, stimulating glycolysis and ATP production[3,23]. Conversely, withdrawal of growth/survival factors decreases the glycolytic rate and O_2 consumption, alters mitochondrial membrane potential, and results in VDAC closure and diminished ADP/ATP exchange[2,3]. Overexpression of anti-apoptotic BCL-2 and BCL-X_L can block the death of cells deprived of growth/survival factors, but does not directly counter the decline in glycolysis[24,25]. These observations suggested that BCL-2 family proteins and glucose metabolism influence cell survival through independent mechanisms. However, our studies of *Bad*$^{-/-}$ and non-phosphorylatable BAD(3SA) cells reveal a unique role

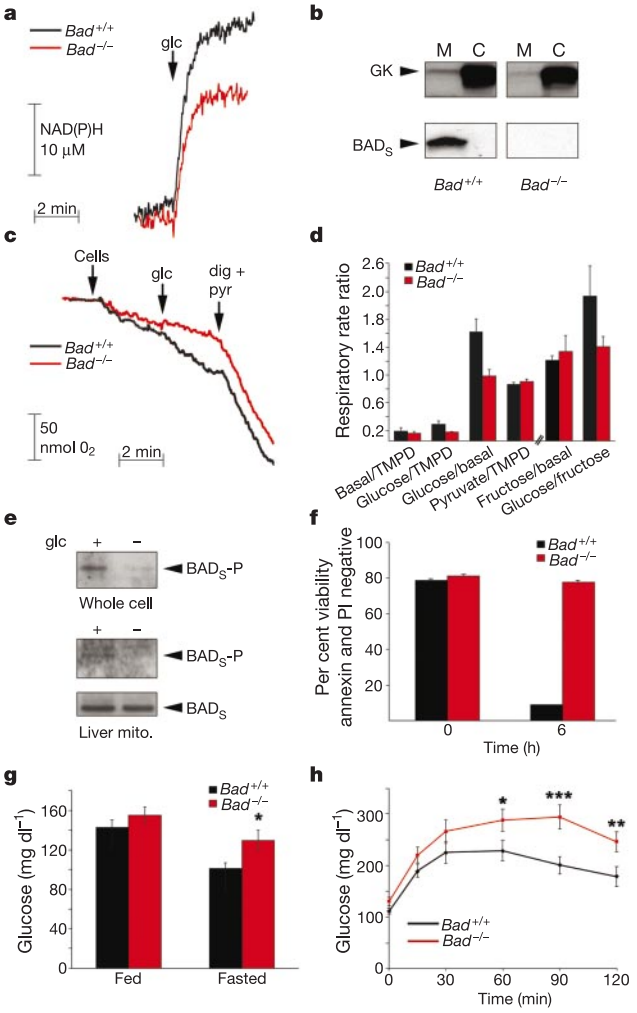

Figure 3 Aberrations in glucokinase activity, glucose homeostasis and glucose-withdrawal-induced cell death in *Bad*$^{-/-}$ mice. **a**, Glucokinase activity in purified liver mitochondria is plotted as glucose-6-phosphate dehydrogenase-driven increase in NAD(P)H fluorescence. Representative trace of multiple independent experiments is shown. **b**, Immunoblot of glucokinase levels in *Bad*$^{+/+}$ and *Bad*$^{-/-}$ mitochondria (M) and cytosol (C) subfractions of liver. **c**, Representative respiratory traces of whole-cell O_2 consumption in response to glucose (glc) or pyruvate-driven respiration comparing *Bad*$^{+/+}$ with *Bad*$^{-/-}$ hepatocytes. Recordings were conducted using a Clark-type oxygen electrode chamber. **d**, Respiratory rate ratios of experiments in **c**. There is a significant difference of *Bad*$^{+/+}$ compared with *Bad*$^{-/-}$ hepatocytes; $P = 0.002$. **e**, Glucose-regulated BAD phosphorylation on S112 (BAD_S-p) in whole-cell lysates of hepatocyte line H4IIE incubated in the presence or absence of glucose (top panel) or in isolated wild-type liver mitochondria treated with glucose *in vitro* (bottom panels). **f**, Viability of cultured hepatocytes shifted from high (22 mM) to low (0.05 mM) glucose medium. **g**, Fed and overnight fasted serum levels of glucose measured in male *Bad*$^{+/+}$ ($n = 5$) and *Bad*$^{-/-}$ ($n = 8$) mice. **h**, Intraperitoneal glucose tolerance test[30] plots the averaged values of three independent experiments performed on male *Bad*$^{+/+}$ ($n = 5$) and *Bad*$^{-/-}$ ($n = 8$) mice. Asterisks in **g**, **h** indicate significant differences of *Bad*$^{-/-}$ compared with Bad$^{-/-}$ mice. Asterisk, $P < 0.05$; double asterisk, $P < 0.01$; triple asterisk, $P < 0.001$, unpaired two-tailed *t*-test.

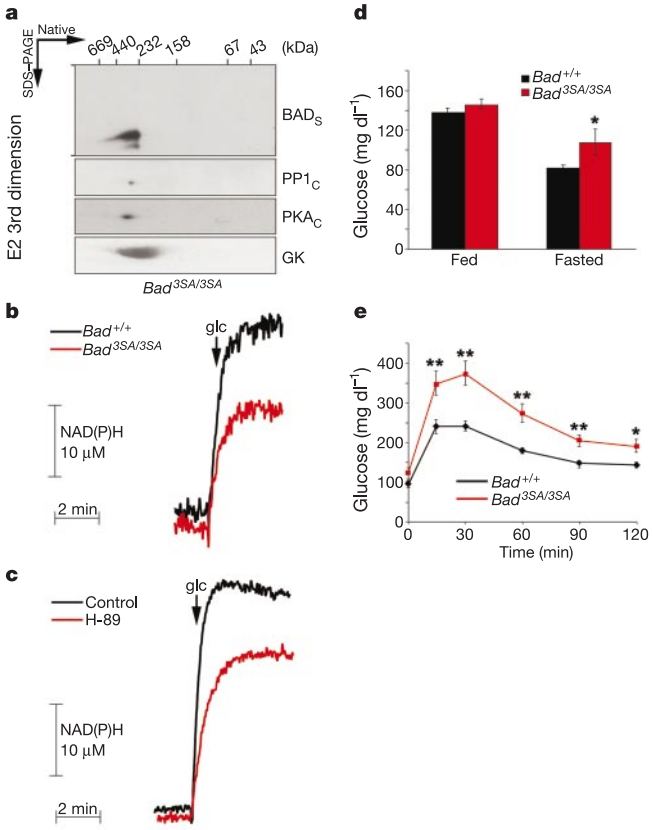

Figure 4 Requirement of BAD phosphorylation in the regulation of mitochondrial glucokinase activity and glucose homeostasis. **a**, The assembly of the mitochondrial BAD complex does not require BAD phosphorylation sites. Third dimension analysis of the BAD complex in *Bad*$^{3SA/3SA}$ liver mitochondria. **b**, Representative plot of mitochondrial glucokinase activity in wild-type compared with *Bad*$^{3SA/3SA}$ liver mitochondria. **c**, Inhibition of mitochondria glucokinase activity by PKA inhibitor H-89. **d**, **e**, Glucose homeostasis in *Bad*$^{3SA/3SA}$ mice. **d**, Fed and overnight fasted serum levels of glucose. **e**, Rate of glucose clearance after intraperitoneal glucose tolerance test measured in male *Bad*$^{+/+}$ ($n = 7$) and *Bad*$^{3SA/3SA}$ ($n = 7$) mice. Asterisks indicate significant differences of *Bad*$^{+/+}$ compared with *Bad*$^{3SA/3SA}$ mice. Asterisk, $P < 0.05$; double asterisk, $P < 0.01$.

for BAD in glucose homeostasis.

The hepatocyte defect and abnormalities in glucose metabolism of *Bad* knockout mice are very similar to a liver-restricted conditional knockout of glucokinase, which demonstrates fasting hyperglycaemia and fed hyperinsulinaemia[21]. This endorses the profound effect of the mitochondria component of glucokinase as essential for proper glucose metabolism. The Michaelis constant (K_m) of glucokinase is close to physiological glucose concentrations, making it an attractive candidate for sensing glucose in this complex. The similarity of *Bad* knockout and knockin mice to diabetic models warrants future, detailed, whole-animal physiological studies, including hyperglycaemic clamps, to define the complete spectrum of systemic changes and compensatory events.

BAD, independent of its phosphorylation status, nucleates a glucokinase-containing complex at the mitochondrion. The Bad^{3SA} allele provides evidence that phosphorylation of BAD is necessary for maximal glucokinase activity, and endorses a kinase–PTPase pair working together within this complex. Notably, the presence of WAVE-1 that controls actin remodelling may relate to the reported actin-dependent organization of glycolytic enzymes, including glucokinase[26], suggesting a rationale for the presence of this particular AKAP in the complex. The striking requirement for BAD in glucose-deprivation-induced death suggests that BAD also serves as an apoptotic sentinel, responding to abnormalities in glucose metabolism. Thus, BH3-only molecules can be integral participants in the pathways that they monitor, ensuring that glycolysis and apoptosis are coordinated. □

Methods

Third dimension analysis of mitochondrial complexes

Mouse liver mitochondria were isolated by standard differential centrifugation (see Supplementary Methods). The procedure described by ref. 27 was adapted as follows. Gel-filtrated mitochondrial proteins were resolved onto 4–12% pre-cast gels (BioRad). Gel lanes were excised and soaked in 2% (w/v) SDS, 0.2 M dithiothreitol (DTT) for 20 min. Each gel strip was layered on top of an 8–16% gradient resolving gel, and a 7% stacking gel poured over and around the native gel slice.

Mass spectrometry

Non-denaturing gels (second dimension; Fig. 1c) or SDS-PAGE gels of microcystin-Sepharose capture assays (Supplementary Fig. 3) were stained either with Coomassie blue or silver stain, and divided horizontally into about ten slices. Resulting gel slices or protein spots from third dimension analysis (Fig. 1e) were individually processed to yield in-gel trypsin digestion products. The resulting peptide mixtures were separated and analysed in an automated system by nanoscale LC-MS/MS on an LCQ-DECA ion trap mass spectrometer (Thermo Finnigan) using the vented-column approach[28] (see Supplementary Methods).

Mitochondrial glucokinase assay

Glucokinase activity was measured spectrophotometrically in a glucose-6-phosphate dehydrogenase-driven NAD(P)H fluorescence assay at 340 nm (ref. 29) with the following modifications. Mouse liver mitochondria (1 mg) were resuspended in 500 μl reaction buffer containing 4 μg ml^{-1} glucose-6-phosphate dehydrogenase, 20 mM $MgCl_2$, 1 mM DTT, 100 mM KCl, 50 mM triethanolamine hydrochloride and 0.1% BSA (see Supplementary Methods).

Microscopy

For confocal microscopy, MEFs were fixed for 20 min at room temperature in PBS containing 3% paraformaldehyde and permeabilized with 0.1% Triton-X100. Incubation with primary and labelled secondary antibodies was performed (see Supplementary Methods for details).

Hepatocyte viability assays

Isolated primary hepatocytes (see Supplementary Methods for details) were resuspended at 6×10^4 cells ml^{-1} in DMEM high glucose medium (22 mM) supplemented with 10 ng ml^{-1} HGF (R&D Systems) or shifted to medium containing HGF but low (0.05 mM) glucose. Viability was assessed by flow cytometric analysis of Annexin-V and propidium iodide staining (Bio Vision).

Mitochondrial respiration assay

Isolated hepatocytes were resuspended in PBS at 5×10^6 cells ml^{-1}, transferred to a Clark-type oxygen electrode chamber (Hansatech), and oxygen consumption recordings were started (see Supplementary Methods for details).

Received 20 March; accepted 27 May 2003; doi:10.1038/nature01825.

1. Raff, M. C. Social controls on cell survival and cell death. *Nature* **356,** 397–400 (1992).
2. Vander Heiden, M. G. *et al.* Growth factors can influence cell growth and survival through effects on glucose metabolism. *Mol. Cell. Biol.* **21,** 5899–5912 (2001).
3. Gottlob, K. *et al.* Inhibition of early apoptotic events by Akt/PKB is dependent on the first committed step of glycolysis and mitochondrial hexokinase. *Genes Dev.* **15,** 1406–1418 (2001).
4. Wang, X. The expanding role of mitochondria in apoptosis. *Genes Dev.* **15,** 2922–2933 (2001).
5. Zha, J., Harada, H., Yang, E., Jockel, J. & Korsmeyer, S. J. Serine phosphorylation of death agonist BAD in response to survival factor results in binding to 14-3-3 not BCL-X(L). *Cell* **87,** 619–628 (1996).
6. Datta, S. R. *et al.* 14-3-3 proteins and survival kinases cooperate to inactivate BAD by BH3 domain phosphorylation. *Mol. Cell* **6,** 41–51 (2000).
7. Harada, H. *et al.* Phosphorylation and inactivation of BAD by mitochondria-anchored protein kinase A. *Mol. Cell* **3,** 413–422 (1999).
8. Harada, H., Andersen, J. S., Mann, M., Terada, N. & Korsmeyer, S. J. p70S6 kinase signals cell survival as well as growth, inactivating the pro-apoptotic molecule BAD. *Proc. Natl Acad. Sci. USA* **98,** 9666–9670 (2001).
9. Moorhead, G., MacKintosh, C., Morrice, N. & Cohen, P. Purification of the hepatic glycogen-associated form of protein phosphatase-1 by microcystin-Sepharose affinity chromatography. *FEBS Lett.* **362,** 101–105 (1995).
10. Westphal, R. S., Soderling, S. H., Alto, N. M., Langeberg, L. K. & Scott, J. D. Scar/WAVE-1, a Wiskott-Aldrich syndrome protein, assembles an actin-associated multi-kinase scaffold. *EMBO J.* **19,** 4589–4600 (2000).
11. Postic, C., Shiota, M. & Magnuson, M. A. Cell-specific roles of glucokinase in glucose homeostasis. *Recent Prog. Horm. Res.* **56,** 195–217 (2001).
12. Datta, S. R. *et al.* Survival factor-mediated BAD phosphorylation raises the mitochondrial threshold for apoptosis. *Dev. Cell* **3,** 631–643 (2002).
13. Wei, M. C. *et al.* Proapoptotic BAX and BAK: a requisite gateway to mitochondrial dysfunction and death. *Science* **292,** 727–730 (2001).
14. Cheng, E. H. *et al.* BCL-2, BCL-X(L) sequester BH3 domain-only molecules preventing BAX- and BAK-mediated mitochondrial apoptosis. *Mol. Cell* **8,** 705–711 (2001).
15. Hsu, Y. T. & Youle, R. J. Bax in murine thymus is a soluble monomeric protein that displays differential detergent-induced conformations. *J. Biol. Chem.* **273,** 10777–10783 (1998).
16. Krimmer, T. *et al.* Biogenesis of porin of the outer mitochondrial membrane involves an import pathway via receptors and the general import pore of the TOM complex. *J. Cell Biol.* **152,** 289–300 (2001).
17. Abdul, K. M. *et al.* Functional analysis of human metaxin in mitochondrial protein import in cultured cells and its relationship with the Tom complex. *Biochem. Biophys. Res. Commun.* **276,** 1028–1034 (2000).
18. Ayllon, V., Martinez, A. C., Garcia, A., Cayla, X. & Rebollo, A. Protein phosphatase 1α is a Ras-activated Bad phosphatase that regulates interleukin-2 deprivation-induced apoptosis. *EMBO J.* **19,** 2237–2246 (2000).
19. Westphal, R. S. *et al.* Regulation of NMDA receptors by an associated phosphatase-kinase signaling complex. *Science* **285,** 93–96 (1999).
20. Machesky, L. M. & Insall, R. H. Scar1 and the related Wiskott-Aldrich syndrome protein, WASP, regulate the actin cytoskeleton through the Arp2/3 complex. *Curr. Biol.* **8,** 1347–1356 (1998).
21. Postic, C. *et al.* Dual roles for glucokinase in glucose homeostasis as determined by liver and pancreatic beta cell-specific gene knock-outs using Cre recombinase. *J. Biol. Chem.* **274,** 305–315 (1999).
22. Bali, D. *et al.* Animal model for maturity-onset diabetes of the young generated by disruption of the mouse glucokinase gene. *J. Biol. Chem.* **270,** 21464–21467 (1995).
23. Cho, H. *et al.* Insulin resistance and a diabetes mellitus-like syndrome in mice lacking the protein kinase Akt2 (PKB beta). *Science* **292,** 1728–1731 (2001).
24. Plas, D. R., Talapatra, S., Edinger, A. L., Rathmell, J. C. & Thompson, C. B. Akt and Bcl-xL promote growth factor-independent survival through distinct effects on mitochondrial physiology. *J. Biol. Chem.* **276,** 12041–12048 (2001).
25. Garland, J. M. & Halestrap, A. Energy metabolism during apoptosis. Bcl-2 promotes survival in hematopoietic cells induced to apoptose by growth factor withdrawal by stabilizing a form of metabolic arrest. *J. Biol. Chem.* **272,** 4680–4688 (1997).
26. Murata, T. *et al.* Co-localization of glucokinase with actin filaments. *FEBS Lett.* **406,** 109–113 (1997).
27. Dekker, P. J. *et al.* The Tim core complex defines the number of mitochondrial translocation contact sites and can hold arrested preproteins in the absence of matrix Hsp70-Tim44. *EMBO J.* **16,** 5408–5419 (1997).
28. Licklider, L. J., Thoreen, C. C., Peng, J. & Gygi, S. P. Automation of nanoscale microcapillary liquid chromatography-tandem mass spectrometry with a vented column. *Anal. Chem.* **74,** 3076–3083 (2002).
29. Niswender, K. D. *et al.* Cell-specific expression and regulation of a glucokinase gene locus transgene. *J. Biol. Chem.* **272,** 22564–22569 (1997).
30. Zhang, C. Y. *et al.* Uncoupling protein-2 negatively regulates insulin secretion and is a major link between obesity, beta cell dysfunction, and type 2 diabetes. *Cell* **105,** 745–755 (2001).

Supplementary Information accompanies the paper on **www.nature.com/nature**.

Acknowledgements We thank M. Ryan, G. Shore, J. Scott, M. Magnuson and B. Spiegelman for reagents; M. Ryan and J. Opferman for technical advice; B. Kahn and O. Peroni for discussion; S. Wade, J. Fisher and J. Sturgill for animal care; U. Maduekwe for technical assistance; and E. Smith for manuscript preparation. N.N.D. is a recipient of the Cancer Research Fund of Damon Runyon Foundation fellowship. This work is supported in part by a NIH grant.

Competing interests statement The authors declare that they have no competing financial interests.

Correspondence and requests for materials should be addressed to S.J.K. (stanley_korsmeyer@dfci.harvard.edu).

